Receding Horizon Estimation and Model Predictive Control for Basic Power Module with High Performance

Liwei Zhou, Matthias Preindl
Department of Electrical Engineering, Columbia University in the City of New York

***Abstract*—A receding horizon estimation (RHE) method is designed in combination with model predictive control (MPC) to improve the dynamic performance of LC-Based Power Module with low cost. Symmetrically mirrored to the MPC, the RHE is configured as a constrained finite time optimal estimation (CFTOE) problem to solve the quadratic cost function based on the past sampling information. An integrated RHE-MPC control method is designed for LC-based power module to formulate power conversion system with high performance. With the designed RHE, the sensor count is reduced with less noise. And the highly accurate RHE contributes to the correction of possible modeling parameters or sampling errors. The integration of RHE and MPC improves the steady state and dynamic performances with less noise, more robust behavior and higher control bandwidth. The proposed methods have been validated experimentally on the power module testbench.**

I. Introduction

STATE estimation is a key part for power electronics to reduce the system cost and improve the dynamic performance. Some conventional estimation methods have been applied in the power converters, such as Luenberger Observer, Kalman Observer and Sliding Mode Observer, etc [1]. The state observers are typically leveraged to estimate the state variables based on the measurement information. An advanced estimation method, called receding horizon estimation (RHE) is designed in this paper combined with the model predictive control (MPC) to improve the steady state/dynamic performances and reduce the sensor count [2].

State estimator is a typical technique to improve the power quality and reduce the cost for power converters. In a power electronics system, the voltage/current samplings are crucial parameters that could directly influence the performance of power control. Due to the hardware limitations, e.g., EMI noise from the high power traces, measurement error, of the sensing circuits, the control system could be interfered by the sampling noise or oscillation. The state estimation can be a substitute for part of the ADC sampling information to reduce the noise/oscillation from the corresponding sensors [3]. Also, the state estimation contributes to the reduction of sensor count and system cost. Conventionally, the Luenberger Observer is a basic state estimation method and has been widely used in the industry applications which is a linear type of observer and can be easily implemented in the digital control systems [4]. Besides the Luenberger Observer, receding horizon estimation (RHE) is a more advanced estimation approach that leverages a series of past measurements to derive the desired accurate state values by solving a constrained optimization problem [5], [6]. The RHE has been verified for the application of virtual flux estimation in electric machine to estimate the position and speed [7], [8]. Few studies have been focusing on the applications of different topologies to be interfaced with wider ranges of load/source. Also, the computation burden for the RHE on low cost DSP is a crucial topic that needs to be addressed for the popularization of the technique. This paper develops a general explicit RHE-MPC method for power modules that could be applied to various types of power converters with different load/source interfaces on a low cost DSP.

Model predictive control (MPC) is an option for the promotion of dynamic performance and resonance damping, especially in high order filter system [9], [10], [11], [12]. Different from the conventional proportional-integral (PI) control, the MPC has been validated to have the advantages of better dynamic performance, including less rising time, overshoot and oscillation during transient [13], [14], [15], [16]. Several MPC algorithms have been studied in the field of power converters for motor traction or grid-connection [17], [18], [19]. However, the combination of MPC and RHE for a general application and low cost implementation purposes have not been addressed in details. The MPC and RHE are actually two symmetrical algorithms in the time series where RHE is focusing on the past sampling information and MPC is for the future steps. This paper integrates the RHE and MPC on a generalized power module which could be applied to various interfaced applications without consuming high computation burden on the controller.

This paper is organized as follows. Firstly, since the combination of RHE and MPC are co-designed with a unified state space model for an LC-based power module, the system modeling of the LC-based power module is introduced. Secondly, the specific RHE and MPC algorithms are analyzed and implemented on the LC-based power module. Finally, the designed RHE and MPC algorithms are validated experimentally on the power module testbench.

II. System Modeling

The system modeling of the LC-based power module is analyzed in this section. The circuitry diagram of the basic LC power module is shown Fig. 1 which consists of upper/lower switches, M_1 and M_2, switch side inductor, L_{fs}, upper/lower

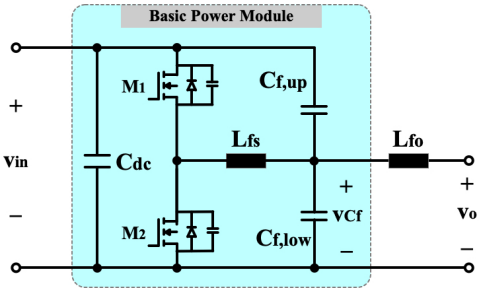

Fig. 1: LC-based power module with output side inductor.

output capacitors, $C_{f,up}$ and $C_{f,low}$. An output side inductor, L_{fo}, can also be connected to formulate an LCL converter. The desired number of introduced basic LC-based power modules can be connected and reconfigured to formulate different types of topological applications such as multi-phase DC/DC or DC/AC converters.

The state space equations for the LC-based power module can be expressed as:

$$\dot{i}_{Lfs}(t) = -\frac{1}{L_{fs}} v_{Cf}(t) + \frac{v_{in}}{L_{fs}} d(t) \tag{1a}$$

$$\dot{v}_{Cf}(t) = \frac{1}{C_f} i_{Lf}(t) - \frac{1}{C_f} i_{Lfo}(t). \tag{1b}$$

$$\dot{i}_{Lfo}(t) = \frac{1}{L_{fo}} v_{Cf}(t) - \frac{1}{L_{fo}} v_o(t). \tag{1c}$$

where L_{fs}, C_f and L_{fo} are the switch side inductor, output capacitor and output side inductor, respectively. i_{Lfs}, v_{Cf}, i_{Lfo} and v_o are the switch side inductor current, output capacitor voltage, output side current and output voltage.

III. Estimation and Control

The proposed integrated receding horizon estimation and model predictive control (RHE-MPC) method for LC-based power module is analyzed in this section. These two advanced techniques are all configured by solving the constrained finite time optimization problems to increase the modeling/sampling accuracy, reduce the hardware cost, enhance the anti-noise capability and improve the steady state/dynamic performances. These two techniques, RHE and MPC, are integrated based on a monolithic state space model of LC power module by dealing with two sets of ADC sampling data. The two sets of sampling data for RHE and MPC are symmetric in time sequences for the past and future, respectively.

A. Receding Horizon Estimation

Different from the traditional Luenberger observer, receding horizon estimation is designed to solve a constrained finite time optimal estimation problem that requires a sequence of past sampling information [20]. The general theory and the implementation for the LC-based power module are analyzed in this section [5], [21].

The RHE method is applied to the LC-based power module for the optimal estimation [22]. Considering the huge current ripple on the switch side inductor current measurement, i_{Lfs},

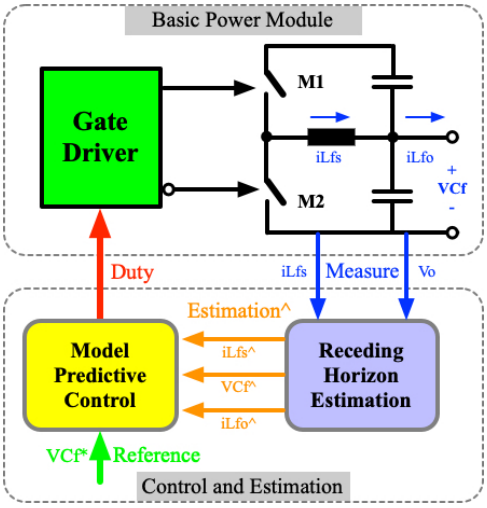

Fig. 2: RHE-MPC Control diagram of LC-based power module.

and the challenges to accurately sample the averaged i_{Lfs},the receding horizon estimator (RHE) is designed for per phase power module to provide more accurate switch side inductor current estimation and noise rejection for the MPC controller [23]. The main purposes of the state estimator are (1) avoid inaccuracy of inductor current sampling with high current ripple; (2) improve the anti-noise capability for better control performance; (3) reduce the sensor cost.

The RHE is implemented by solving the *Constrained Finite Time Optimal Estimation* (CFTOE) problem to derive the optimal estimated values of switch side inductor current, $\hat{i}_{Lfs}$, capacitor voltage, $\hat{v}_{Cf}$, and grid side inductor current, $\hat{i}_{Lfo}$, with the samplings of capacitor voltage, v_{Cf}, and grid side inductor current, i_{Lfo}. The state-space equations for the discrete-time RHE can be expressed in standard matrix format of

$$\hat{X}_{k+1} = A_E \hat{X}_k + B_E u_k \tag{2a}$$

$$\hat{Y}_k = C_E \hat{X}_k + D_E u_k \tag{2b}$$

where the variables and matrices for RHE represent

$$A_E = \begin{bmatrix} 0 & -\frac{T_s}{L_{fs}} & 0 \\ \frac{T_s}{C_f} & 0 & -\frac{T_s}{C_f} \\ 0 & 0 & 0 \end{bmatrix}, B_E = \begin{bmatrix} \frac{T_s}{L_{fs}} \\ 0 \\ 0 \end{bmatrix}, \tag{3a}$$

$$C_E = \begin{bmatrix} 0 & 1 & 0 \\ 0 & 0 & 1 \end{bmatrix}, D_E = \begin{bmatrix} 0 \\ 0 \end{bmatrix}, \tag{3b}$$

$$\hat{X}_k = \begin{bmatrix} \hat{i}_{Lfs}(k) \\ \hat{v}_{Cf}(k) \\ \hat{i}_{Lfo}(k) \end{bmatrix}, \hat{Y}_k = \begin{bmatrix} \hat{v}_{Cf}(k) \\ \hat{i}_{Lfo}(k) \end{bmatrix}. \tag{3c}$$

Based on the RHE state-space equations in (2), the RHE solves for the optimal estimated state variable sequence of $\hat{X}_M, ..., \hat{X}_0$ with the known past measurement sampling sequence of $Y_M, ..., Y_0$ and input variable sequence of $u_M, ..., u_{-1}$. The cost function of RHE optimization problem is composed of two parts:

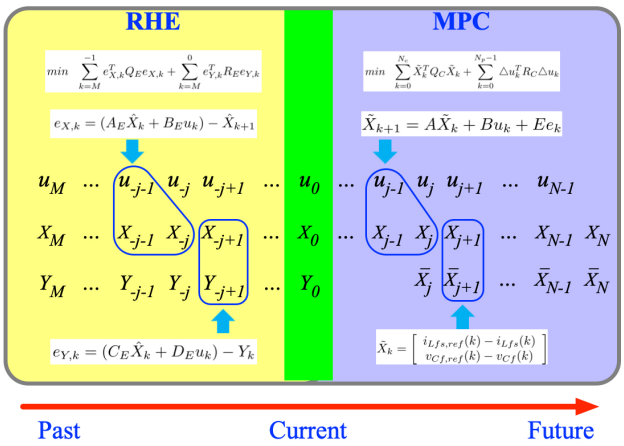

Fig. 3: Relationship between receding horizon estimation and model predictive control.

(1) Minimization of error between state equation (2a) and estimated state variable $\hat{X}_{j+1}$ which can be expressed as

$$e_{X,k} = (A_E\hat{X}_k + B_E u_k) - \hat{X}_{k+1}; \tag{4}$$

(2) Minimization of error between state equation (2b) and measured sampling output variable Y_j which can be expressed as

$$e_{Y,k} = (C_E\hat{X}_k + D_E u_k) - Y_k. \tag{5}$$

Thus, the RHE cost function for the CFTOE optimization can be expressed as

$$min \quad \sum_{k=M}^{-1} e_{X,k}^T Q_E e_{X,k} + \sum_{k=M}^{0} e_{Y,k}^T R_E e_{Y,k} \tag{6}$$

where Q_E and R_E represent the weighing factor matrices of the penalties that are implemented on the state variables and output variables, respectively.

The constraints of the RHE controller can be expressed as

$$e_{X,k} = (A_E\hat{X}_k + B_E u_k) - \hat{X}_{k+1} \in \mathcal{E}_{\mathcal{X}} \tag{7}$$

$$e_{Y,k} = (C_E\hat{X}_k + D_E u_k) - Y_k \in \mathcal{E}_{\mathcal{Y}} \tag{8}$$

$$\begin{bmatrix} -I_{Lfs,max} \\ 0 \\ -I_{Lfo,max} \end{bmatrix} \leq \hat{X}_k \leq \begin{bmatrix} I_{Lfs,max} \\ v_{in} \\ I_{Lfo,max} \end{bmatrix} \tag{9}$$

$$\begin{bmatrix} 0 \end{bmatrix} \leq u_k \leq \begin{bmatrix} v_{in} \end{bmatrix} \tag{10}$$

$$\begin{bmatrix} 0 \\ -I_{Lfo,max} \end{bmatrix} \leq Y_k \leq \begin{bmatrix} v_{in} \\ I_{Lfo,max} \end{bmatrix}. \tag{11}$$

The working mechanisms of RHE and MPC are symmetrical with respect to the present state. Specifically, RHE is dealing with the states from past to present steps and MPC is optimizing the states from present to the future steps. The relationship between RHE and MPC has been shown in Fig. 3.

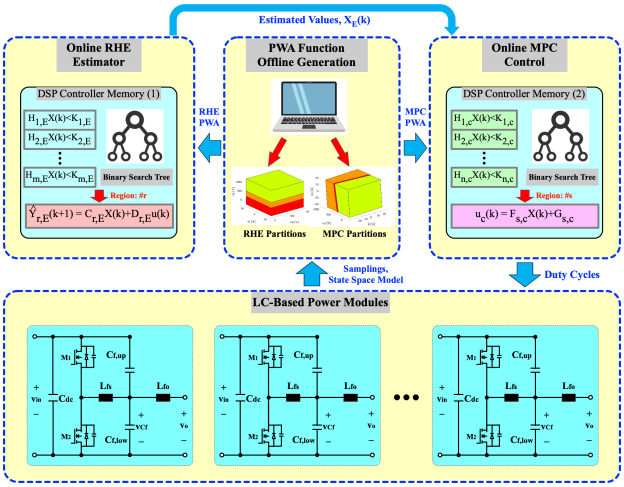

Fig. 4: Explicit implementation of RHE and MPC with online search tree.

B. Model Predictive Control

The MPC algorithm is derived by solving the constrained finite time optimal control (CFTOC) problem [24]. A cost function can be configured to minimize the tracking error between the state variable vector, $x(k)$, and the references, $\overline{x}(k)$, by predicting a series of future input variable, $u(k)$ [25]. The cost function can be generally expressed as:

$$\underset{\substack{x(1),\ldots,x(N)\\ u(1),\ldots,u(N-1)}}{\text{argmin}} \sum_{k=0}^{N-1} e_{x,k}^T \mathbf{Q}_C e_{x,k} + \sum_{k=0}^{N-1} e_{u,k}^T \mathbf{R}_C e_{m,k} + e_{u,N}^T \mathbf{P}_C e_{x,N}. \tag{12}$$

And the constraints are followed by:

$$s.t. \quad e_{x,k} = \overline{x}(k) - x(k) \tag{13a}$$

$$e_{u,k} = u(k) - u(k-1) \tag{13b}$$

$$x(k) \in \mathcal{X} \tag{13c}$$

$$u(k) \in \mathcal{U} \tag{13d}$$

where $k > 0$ in (12) and (13) means the information are expected for the prediction of the future instants. The weighing matrices, $\mathbf{Q}_C$ and $\mathbf{R}_C$, provide the penalties on the tracking errors and control input variations, respectively. The matrix, $\mathbf{P}_C$, is defined as the terminal cost which is a basic term in MPC that connects the properties between the finite time MPC and the infinite time LQR. The terminal cost is used to make sure of the stability, robustness and convergence.

IV. Capacitor and Inductor Design for Stability

The capacitor and inductor values design for the filtering circuit are analyzed in this section. The main standard that needs to follow is the grid current/voltage waveforms quality [26], [27]. The specification can be found from IEEE STD 519 to choose the value of grid side inductor, L_g, for the attenuation grid current harmonics.

For the switch side inductor, the minimum inductance, $L_{f,min}$, can be determined by the maximum required current

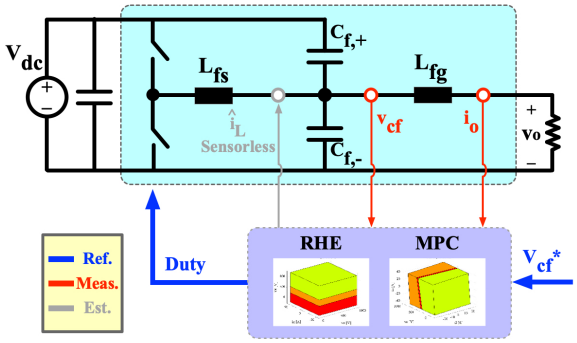

Fig. 5: The integrated RHE and MPC control diagram for the DC/DC interfaced application with LC-based power module.

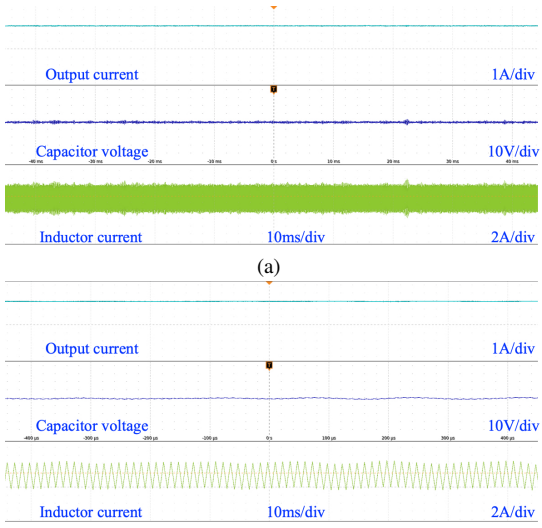

Fig. 6: RHE-MPC (a) experimental and (b) zoomed waveforms of output current, capacitor voltage, inductor current for DC/DC converter.

ripple, $\Delta i_{L,max}$, with the duty cycle of 0.5, d, switching frequency, f_{sw}, and DC bus voltage, V_{dc}

$$L_{f,min} = \frac{d(1-d)V_{dc}}{f_{sw}\Delta i_L}. \tag{14}$$

With the desired grid/switch side inductance determined, the capacitance can be designed by the minimum output voltage ripple, u_{ripple} and the resonant frequency of the LCL filter, ω_{res}. Specifically, the minimum capacitance is determined by the output voltage ripple which is expressed as

$$C_{f,up,min} + C_{f,lo,min} = \frac{1 - d_{min}}{8L_f u_{ripple}[\%] f_{sw}^2}. \tag{15}$$

Then, from the minimum available $C_{f,up,min}$ and $C_{f,lo,min}$, the value of capacitance can be adjusted to determine the resonant frequency of LCL filter system as is shown in

$$\omega_{res} = \sqrt{\frac{L_f + L_g}{L_f L_g (C_{f,up} + C_{f,lo})}}. \tag{16}$$

Based on (16), the capacitor values can be finally determined to choose a specific resonant frequency of the LCL filter.

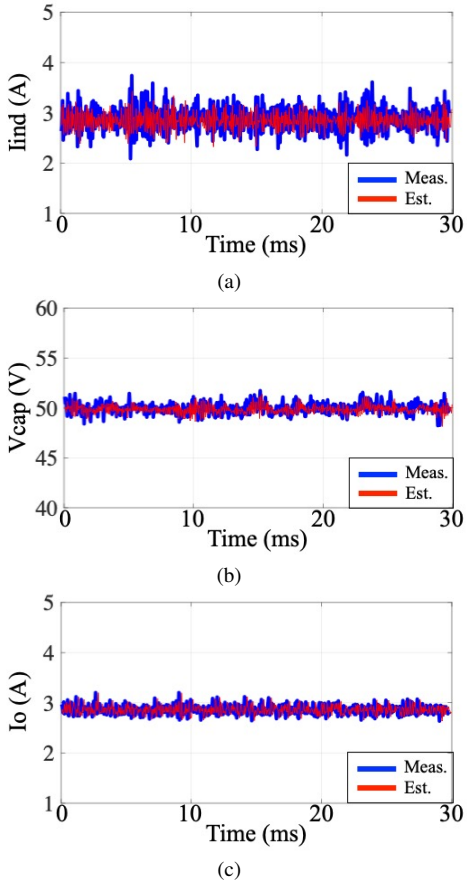

Fig. 7: RHE estimation performance of the experimentally captured steady state ADC readings of measurement and estimation for grid-interfaced (a) inductor current (b) capacitor voltage and (c) grid current.

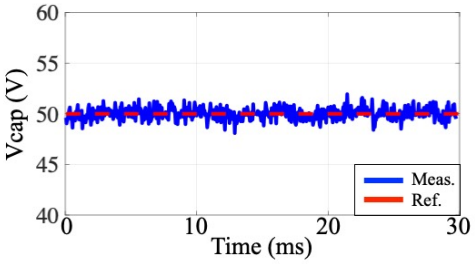

Fig. 8: MPC tracking performance of the experimentally captured steady state ADC readings of capacitor voltage for the DC/DC application.

Then, with the help of ω_{res} and LCL parameters, the control bandwidth, ω_c, can be further designed to avoid the excitation.

V. Applications and Results

The application for the developed RHE-MPC technique in DC/DC interfaced power converter in Fig. 5 is tested experimentally. The combined RHE-MPC algorithms are configured in the LC-based power module to control the output voltage, v_o. Specifically, the output capacitor voltage, v_{Cf}, and output current, i_o, are directly measured as the output variable matrix,

Y_k, in (2). The inductor current, $\hat{i_L}$, output capacitor voltage, $\hat{v_{Cf}}$, and output current, $\hat{i_o}$, are configured as the estimated state variable matrix, $\hat{X_k}$. Based on the RHE cost function in (6) and the corresponding constraints in (7)-(11) to deal with the past sampling information within the estimation horizon, the optimal estimation of $\hat{X_k}$ will be derived for the purpose of MPC control process with less noise.

Symmetrically with RHE, the MPC manages the future sampling information within the prediction horizon to derive the optimal input variable matrix, u_k, of duty cycle by solving the MPC cost function and the corresponding constriants. Instead of using the noisy sampling state variables of X_k, the MPC utilizes the estimated state variables, $\hat{X_k}$, from RHE to track the output capacitor voltage reference with less noise and oscillation.

Fig. 6 shows the output current, capacitor voltage and inductor current waveforms of the DC/DC converter with RHE-MPC method. The DC/DC application results demonstrate that RHE can reduce the noise and oscillation. Furthermore, for the DC/DC application, the experimentally captured ADC readings of measurement and estimation for inductor current, capacitor voltage and output current are shown in Fig. 7. Fig. 8 shows the MPC reference and measurement for DC/DC converter output capacitor voltage where the MPC accurately tracks a voltage reference of 50V. The sampling noise from sensor is largely reduced by RHE for a more stable performance.

VI. Conclusion

This paper developed a RHE-MPC combined algorithm to improve the steady state/dynamic performance of an LC-based power module. The general theories of RHE and MPC are introduced. The developed algorithms are implemented on a DC/DC application by connecting the LC-based power modules with a resistive load. Half of the current sensors are saved with the RHE method. The experimental results show the RHE and MPC have good anti-noise capability.

References

[1] M. Hinkkanen and J. Luomi, "Modified integrator for voltage model flux estimation of induction motors," *IEEE Transactions on Industrial Electronics*, vol. 50, no. 4, pp. 818–820, 2003.

[2] L. Zhou, M. Jahnes, M. Eull, W. Wang, G. Cen, and M. Preindl, "Robust control design for ride-through/trip of transformerless onboard bidirectional ev charger with variable-frequency critical-soft-switching," *IEEE Transactions on Industry Applications*, pp. 1–1, 2022.

[3] G. Rinaldi, P. P. Menon, C. Edwards, and A. Ferrara, "Design and validation of a distributed observer-based estimation scheme for power grids," *IEEE Transactions on Control Systems Technology*, vol. 28, no. 2, pp. 680–687, 2020.

[4] Z. Yin, C. Bai, N. Du, C. Du, and J. Liu, "Research on internal model control of induction motors based on luenberger disturbance observer," *IEEE Transactions on Power Electronics*, vol. 36, no. 7, pp. 8155–8170, 2021.

[5] A. Alessandri, M. Baglietto, and G. Battistelli, "Receding-horizon estimation for switching discrete-time linear systems," *IEEE Transactions on Automatic Control*, vol. 50, no. 11, pp. 1736–1748, 2005.

[6] K. Ling and K. Lim, "Receding horizon recursive state estimation," *IEEE Transactions on Automatic Control*, vol. 44, no. 9, pp. 1750–1753, 1999.

[7] Z. Yin, Y. Zhang, C. Du, J. Liu, X. Sun, and Y. Zhong, "Research on anti-error performance of speed and flux estimation for induction motors based on robust adaptive state observer," *IEEE Transactions on Industrial Electronics*, vol. 63, no. 6, pp. 3499–3510, 2016.

[8] J.-N. Shen, J.-J. Shen, Y.-J. He, and Z.-F. Ma, "Accurate state of charge estimation with model mismatch for li-ion batteries: A joint moving horizon estimation approach," *IEEE Transactions on Power Electronics*, vol. 34, no. 5, pp. 4329–4342, 2019.

[9] A. G. Beccuti, M. Kvasnica, G. Papafotiou, and M. Morari, "A decentralized explicit predictive control paradigm for parallelized dc-dc circuits," *IEEE Transactions on Control Systems Technology*, vol. 21, no. 1, pp. 136–148, 2013.

[10] S. Almér, S. Mariéthoz, and M. Morari, "Dynamic phasor model predictive control of switched mode power converters," *IEEE Transactions on Control Systems Technology*, vol. 23, no. 1, pp. 349–356, 2015.

[11] S.-K. Kim, C. R. Park, J.-S. Kim, and Y. I. Lee, "A stabilizing model predictive controller for voltage regulation of a dc/dc boost converter," *IEEE Transactions on Control Systems Technology*, vol. 22, no. 5, pp. 2016–2023, 2014.

[12] L. Zhou, M. Jahnes, M. Eull, W. Wang, and M. Preindl, "Control design of a 99% efficiency transformerless ev charger providing standardized grid services," *IEEE Transactions on Power Electronics*, vol. 37, no. 4, pp. 4022–4038, 2022.

[13] A. Bemporad, F. Borrelli, and M. Morari, "Model predictive control based on linear programming - The explicit solution," *IEEE Transactions on Automatic Control*, vol. 47, no. 12, pp. 1974–1985, 2002.

[14] Y. Xie, R. Ghaemi, J. Sun, and J. S. Freudenberg, "Model predictive control for a full bridge dc/dc converter," *IEEE Transactions on Control Systems Technology*, vol. 20, no. 1, pp. 164–172, 2012.

[15] M. Eull, L. Zhou, M. Jahnes, and M. Preindl, "Bidirectional nonisolated fast charger integrated in the electric vehicle traction drivetrain," *IEEE Transactions on Transportation Electrification*, vol. 8, no. 1, pp. 180–195, 2022.

[16] L. Zhou and M. Preindl, "Variable-switching constant-sampling frequency critical soft switching mpc for dc/dc converters," *IEEE Transactions on Energy Conversion*, vol. 36, no. 2, pp. 1548–1561, 2021.

[17] Y. Yang, S.-C. Tan, and S. Y. R. Hui, "Adaptive reference model predictive control with improved performance for voltage-source inverters," *IEEE Transactions on Control Systems Technology*, vol. 26, no. 2, pp. 724–731, 2018.

[18] X. Liu, D. Wang, and Z. Peng, "Cascade-free fuzzy finite-control-set model predictive control for nested neutral point-clamped converters with low switching frequency," *IEEE Transactions on Control Systems Technology*, vol. 27, no. 5, pp. 2237–2244, 2019.

[19] L. Zhou and M. Preindl, "Optimal tracking and resonance damping design of cascaded modular model predictive control for common-mode stabilized grid-tied lcl inverter," *IEEE Transactions on Power Electronics*, pp. 1–1, 2022.

[20] Y. Wang and Z. Deng, "Improved stator flux estimation method for direct torque linear control of parallel hybrid excitation switched-flux generator," *IEEE Transactions on Energy Conversion*, vol. 27, no. 3, pp. 747–756, 2012.

[21] T. Ouyang, P. Xu, J. Chen, J. Lu, and N. Chen, "An online prediction of capacity and remaining useful life of lithium-ion batteries based on simultaneous input and state estimation algorithm," *IEEE Transactions on Power Electronics*, vol. 36, no. 7, pp. 8102–8113, 2021.

[22] L. Y. Wang, F. Lin, and W. Chen, "Controllability, observability, and integrated state estimation and control of networked battery systems," *IEEE Transactions on Control Systems Technology*, vol. 26, no. 5, pp. 1699–1710, 2018.

[23] M. Z. El-Sharafy, S. Saxena, and H. E. Farag, "Optimal design of islanded microgrids considering distributed dynamic state estimation," *IEEE Transactions on Industrial Informatics*, vol. 17, no. 3, pp. 1592–1603, 2021.

[24] S. Yu, T. Fernando, H. H.-C. Iu, and K. Emami, "Realization of state-estimation-based dfig wind turbine control design in hybrid power systems using stochastic filtering approaches," *IEEE Transactions on Industrial Informatics*, vol. 12, no. 3, pp. 1084–1092, 2016.

[25] H. T. Nguyen and J. W. Jung, "Finite control set model predictive control to guarantee stability and robustness for surface-mounted PM synchronous motors," *IEEE Transactions on Industrial Electronics*, vol. 65, no. 11, pp. 8510–8519, 2018.

[26] L. Zhou and M. Preindl, "Inductor design for nonisolated critical soft switching converters using solid and litz pcb and wire windings leveraging neural network model," *IEEE Transactions on Power Electronics*, vol. 37, no. 3, pp. 3357–3373, 2022.

[27] B. Agrawal, L. Zhou, A. Emadi, and M. Preindl, "Variable-frequency critical soft-switching of wide-bandgap devices for efficient high-frequency nonisolated dc-dc converters," *IEEE Transactions on Vehicular Technology*, vol. 69, no. 6, pp. 6094–6106, 2020.